

Dinuclear Gold Diselenophosphate Complexes: Structures and Photoluminescence

Hong-Jhin You,[†] Ching-Shiang Fang,[†] Ju-Ling Lin,[‡] Shih-Sheng Sun,^{*,‡} and C. W. Liu^{*,†}

[†]Department of Chemistry, National Dong Hwa University, Hualien, Taiwan 97401, Republic of China, and

[‡]Institute of Chemistry, Academia Sinica, Taipei, Taiwan 115, Republic of China

Received July 13, 2010

Structures of $[\text{AuSe}_2\text{P}(\text{OR})_2]_2$ ($\text{R} = \text{}^i\text{Pr}$, **1**; Et, **2**), the first homoleptic dinuclear gold(I) bridged by phosphorodiselenoates, are reported along with their intriguing photoluminescent properties, which display multiple emissions as well as thermochromism.

The majority of homo- and heterodinuclear gold(I) complexes are bridged by carbon-, nitrogen-, phosphorus-, and sulfur-donor ligands.¹ The facile oxidative addition reaction on the gold(I) ylide dimers² in the formation of the Au–Au bond coupled with the rich photophysical properties revealed in most of the dinuclear gold compounds,³ which normally display comparable inter- and intramolecular Au–Au distances (a representation of aurophilic contact⁴), continues to blossom gold chemistry. On the other hand, dinuclear gold(I) complexes with selenium-donor ligands are comparably less studied.⁵ Surprisingly, structurally characterized, gold(I) dimers with each gold center coordinated by two selenium atoms of the selenoorganophosphorus moiety, to the best of our knowledge, have never been reported⁶ even though a number of selenium-bound, heteroleptic dinuclear gold complexes have been prepared using a diselenoimidodiphosphinato anion

$[\text{R}_2\text{P}(\text{Se})\text{NP}(\text{Se})\text{R}_2]^-$,⁷ phenylselenolato (PhSe^-),⁸ 1,4-phenylenediselenolato,⁹ selenourea,¹⁰ and selenocarbamate ester¹¹ as ligands. The solid-state structure of $[\text{Au}_2\{\text{Se}_2\text{CC}(\text{CN})_2\}_2]^{2-}$ is elusive, however.¹²

Over the years, our research group has had profound interest in the development of the coordination chemistry of diselenophosphate (dsep) ligands.¹³ Both tetranuclear copper(I) and hexanuclear silver(I) clusters supported by *O,O'*-diisopropyl diselenophosphates,¹⁴ of which structural characteristics show a great resemblance to their sulfur counterparts,¹⁵ have been demonstrated. Along this line, it is natural to generate Au^Idsep complexes inspired by both the limited examples of structurally characterized digold compounds with selenium-donor ligands and the rich photophysics of digold–sulfur complexes such as $[\text{AuS}_2\text{P}(\text{OME})_2]_2$,¹⁶ which display multiple emitting states including both singlet and triplet metal-centered (MC; $d_{z^2}\sigma^* \rightarrow p_z\sigma$) states and a ligand-to-metal charge-transfer (LMCT; $\text{S } p \rightarrow \text{Au } p_z\sigma$) state. Herein we report the synthesis and structure of $[\text{AuSe}_2\text{P}(\text{OR})_2]_2$ ($\text{R} = \text{}^i\text{Pr}$, **1**; Et, **2**), the first homoleptic dinuclear gold(I) bridged by dialkyl diselenophosphates, and their photoluminescent properties.

The dimetallic gold(I) complexes $[\text{AuSe}_2\text{P}(\text{OR})_2]_2$ ($\text{R} = \text{}^i\text{Pr}$, **1**; Et, **2**) were obtained as yellow powders from the reaction of $\text{AuCl}(\text{THF})$ with a stoichiometric amount of $\text{NH}_4[\text{Se}_2\text{P}(\text{OR})_2]$

*To whom correspondence should be addressed. E-mail: sssun@chem.sinica.edu.tw (S.-S.S.), chenwei@mail.ndhu.edu.tw (C.W.L.).

(1) (a) Gimeno, M. C.; Laguna, A. In *Comprehensive Coordination Chemistry II*; McCleverty, J. A., Meyer, T. J., Eds.; Elsevier: Oxford, U.K., 2004; Vol. 6, p 911. (b) Mohamed, A. A.; Abdou, H. E.; Fackler, J. P., Jr. *Coord. Chem. Rev.* **2010**, *254*, 1253–1259.

(2) Grohmann, A.; Schmidbaur, H. In *Comprehensive Organometallic Chemistry II*; Abel, E. W., Stone, F. G. A., Wilkinson, G., Eds.; Elsevier: Oxford, U.K., 1995; Vol. 3, p1.

(3) (a) Lopez-de-Luzuriaga, J. M. In *Modern Supramolecular Gold Chemistry: Gold–Metal Interactions and Applications*; Laguna, A., Ed.; Wiley-VCH: Weinheim, Germany, 2008; Chapter 6, p 347. (b) Yam, V. W.-W.; Cheng, E. C.-C. *Chem. Soc. Rev.* **2008**, *37*, 1806–1813. (c) van Zyl, W. E.; López-de-Luzuriaga, J. M.; Mohamed, A. A.; Staples, R. J.; Fackler, J. P., Jr. *Inorg. Chem.* **2002**, *41*, 4579–4589. (d) van Zyl, W. E. *Comments Inorg. Chem.* **2010**, *31*, 13–32.

(4) (a) Pykkö, P. *Chem. Rev.* **1997**, *97*, 597–636. (b) Schmidbaur, H. *Chem. Soc. Rev.* **1995**, *24*, 391–400.

(5) Mohr, F.; Molter, A. *Coord. Chem. Rev.* **2010**, *254*, 19–45.

(6) Dinuclear gold(I) compounds connected by polyselenides such as $[\text{Au}_2(\text{Se}_2)(\text{Se}_4)]^{2-}$,^a $[\text{Au}_2(\text{Se}_2)(\text{Se}_3)]^{2-}$,^a and $[\text{Au}_2(\text{TeSe}_2)]^{2-}$ ^b are known. (a) Huang, S.-P.; Kanatzidis, M. G. *Inorg. Chem.* **1991**, *30*, 3572–3575. (b) Dibrov, S. M.; Ibers, J. A. *Chem. Commun.* **2003**, 2158–2159.

(7) Wilton-Ely, J. D. E. T.; Schier, A.; Schmidbaur, H. *Inorg. Chem.* **2001**, *40*, 4656–4661.

(8) Eiken, W.; Keinitz, C.; Jones, P. G.; Thone, C. *J. Chem. Soc., Dalton Trans.* **1994**, 83–90.

(9) Taher, D.; Taylor, N. J.; Corrigan, J. F. *Can. J. Chem.* **2009**, *87*, 380–385.

(10) Jones, P. G.; Thine, C. *Chem. Ber.* **1991**, *124*, 2725–2729.

(11) Gallenkamp, D.; Porsch, T.; Molter, A.; Tiekink, E. R.; Mohr, F. *J. Organomet. Chem.* **2009**, *694*, 2380–2385.

(12) Dietzsch, W.; Franke, A.; Hoyer, E.; Gruss, D.; Hummel, H. U.; Otto, P. *Z. Anorg. Allg. Chem.* **1992**, *611*, 81–84. No full structure solution, except unit cell parameters, was reported.

(13) Lobana, T. S.; Wang, J.-C.; Liu, C. W. *Coord. Chem. Rev.* **2007**, *251*, 91–110.

(14) (a) Hsu, Y.-J.; Hung, C.-M.; Lin, Y.-F.; Liaw, B.-J.; Lobana, T. S.; Lu, S.-Y.; Liu, C. W. *Chem. Mater.* **2006**, *18*, 3323–3329. (b) Liu, C. W.; Shang, I.-J.; Hung, C.-M.; Wang, J.-C.; Keng, T.-J. *J. Chem. Soc., Dalton Trans.* **2002**, 1974–1979.

(15) (a) Lawton, S. J.; Rohrbaugh, W. J.; Kokotailo, G. T. *Inorg. Chem.* **1972**, *11*, 612–618. (b) Liu, C. W.; Pitts, J. T.; Fackler, J. P., Jr. *Polyhedron* **1997**, *16*, 3899–3909.

(16) Lee, Y. A.; McGarrah, J. E.; Lachicotte, R. J.; Eisenberg, R. *J. Am. Chem. Soc.* **2002**, *124*, 10662–10663.

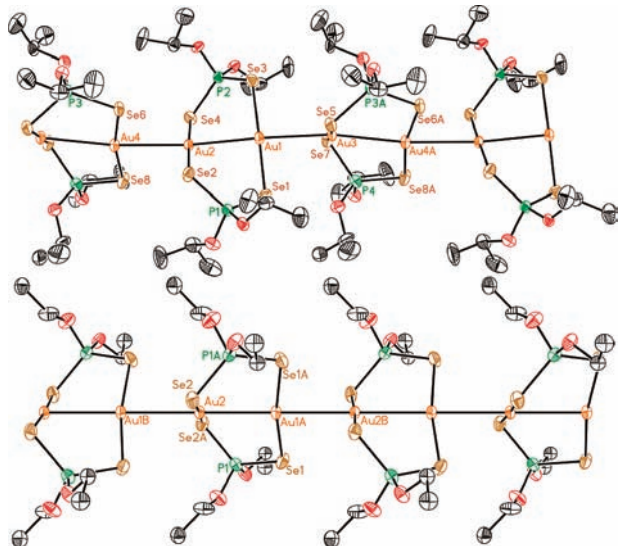


Figure 1. Perspective views of **1** (top) and **2** (bottom). Selected interatomic distances (Å) and angles (deg): **1**, Au1–Au2, 2.9455(9); Au1–Au3, 3.0170(9); Au2–Au4, 3.0681(9); Au3–Au4A, 3.0843(9); Se3–Au1–Se1, 178.91(5); Se4–Au2–Se2, 178.21(5); Se5–Au3–Se7, 173.18(4); Se6–Au4–Se8, 166.89(5); Au1–Au3–Au4A, 171.39(3); Au2–Au1–Au3, 174.13(3) [symmetry code: A, 1 + X, Y, Z]; **2**, Au1A–Au2, 2.9434(9); Au1A–Au2B, 3.0325(9); Se1–Au1A–Se1A, 169.21(14); Se2–Au2–Se2A, 176.31(14); Au2–Au1A–Au2B, 180.0 [symmetry code: A, –X, –Y, Z; B, X, –Y, $\frac{1}{2} + Z$].

over the course of 4 h in tetrahydrofuran (THF) at $-50\text{ }^{\circ}\text{C}$ under a nitrogen atmosphere. Both compounds were characterized by standard analytical/spectroscopic techniques, and the solid-state structures were determined by single-crystal X-ray diffraction (Figure 1).¹⁷ Although attempts to crystallize the complexes at room temperature resulted in decomposition of the compounds to an insoluble black powdery material, single crystals appropriate for X-ray diffraction could only be grown at low temperature. Both complexes are isostructural and closely resemble their sulfur analogues, $[\text{Au}_2\text{P}(\text{OR})_2]_2$ ($\text{R} = \text{Et}^{16}$ and Pr^{18}). In the solid state, both compounds are built into a one-dimensional chain based on the near-colinear alignment of dimetalacycle entities, $[\text{Au}_2\{\text{Se}_2\text{P}(\text{OR})_2\}]_2$, with shorter intramolecular and slightly longer intermolecular Au–Au distances. The gold centers in a $[\text{AuSe}_2\text{P}(\text{OR})_2]_2$ basic unit are doubly bridged by two selenium atoms of dsep ligands, resulting in a puckered eight-membered ring with a short transannular Au \cdots Au interaction. The Au–Se distances [2.408 Å (av.) for **1** and 2.412 Å (av.) for **2**] fall well within the range of those reported values, 2.390(1) Å (av.) for $[\text{Au}(\text{SeCF}_3)_2]^{19}$ and 2.424(1) (av.) Å for $[\{\text{N}(\text{Ph}_2\text{PSe})_2\text{-Se,Se'}\}\text{Au}_2(\text{dppm})\}^+$.⁷ While Se–Au–Se angles, 169.2(1) $^{\circ}$ and 176.3(2) $^{\circ}$ for **2**, deviate from linear-

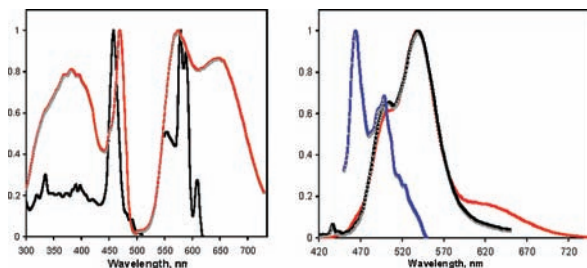


Figure 2. (Left, a) Normalized excitation and emission spectra of compounds **1** (black curve) and **2** (red curve) in the solid state at 77 K. (Right, b) Normalized emission spectra of complex **1** in 2-MeTHF glass at 77 K: blue curve, 3.3×10^{-5} M; black curve, 5.1×10^{-4} M; red curve, 3.4×10^{-3} M.

ity, those in **1** [178.9(0) $^{\circ}$, 178.2(2) $^{\circ}$, 166.8(8) $^{\circ}$, and 173.9(5) $^{\circ}$] are also not strictly linear. The latter leads to Au–Au–Au angles of 171.4(3) $^{\circ}$ and 174.1(3) $^{\circ}$; the former displays a strict linear Au–Au–Au chain. While in compound **2** the intra- and intermolecular Au \cdots Au distances, 2.9434(9) and 3.0325(9) Å, respectively, are invariant, the Au \cdots Au distances in **1** [intramolecular, 2.9455(9) and 3.0843(9) Å; intermolecular, 3.0170(9) and 3.0681(9) Å] are varied to a lesser extent. The differences in the Au \cdots Au distances are perhaps due to the molecular packing and associated van der Waals forces as reported for $[\text{AuS}_2\text{P}(\text{O}^i\text{Pr})_2]_2$ by Lawton et al.¹⁸ The adjacent dimeric units of compounds **1** and **2** in a one-dimensional chain are rotated by ca. 67.1 $^{\circ}$ and 72.1 $^{\circ}$, respectively, along the Au \cdots Au direction to minimize non-bonding repulsions between adjacent ligands. To date, only a limited number of dinuclear gold compounds comprising bridging selenium-donor ligands have been synthesized.^{6–12} The compound $[\text{Au}\{\text{N}(\text{Ph}_2\text{PSe})_2\}]_2$, which exhibited poor solubility in common laboratory solvents, was proposed as a polymeric species in the solid state.⁷ Thus, to the best of our knowledge, no structural information is available on gold(I) compounds containing Se–P–Se bridging ligands prior to this report.

Photophysical data of compounds **1** and **2** are summarized in Table S1 in the Supporting Information. The electronic spectral profiles of **1** and **2** in THF are very similar. The spectra display two shoulder absorptions at about 281–284 and 341–345 nm ($\epsilon = 710\text{ M}^{-1}\text{ cm}^{-1}$). The origin of the high-energy shoulder is presumably a ligand-centered transition because the free ligand displayed absorptions in similar regions.²⁰ The low-energy shoulder is tentatively assigned to the MC transition, where the permitted electronic transition of gold(I), $^1\text{S}_0 \rightarrow ^1\text{D}_0$, in gaseous ions is 29 620 cm^{-1} (338 nm) above the ground state.²¹ Both compounds exhibit weak orange emissions in the solid state at room temperature, and the emission color becomes intense at 77 K (Figure 2a). The emission maxima appeared at 580 and 575 nm for **1** and **2**, respectively. The distinct vibronic feature with an average 510 cm^{-1} vibrational spacing of the emission spectrum for complex **1** indicates a ligand-perturbed excited state involved in the emissive states.²² The excited-state lifetime of compound **1**

(17) Crystal data for **1**: monoclinic, $P2_1/n$, $a = 12.078(2)$ Å, $b = 22.850(4)$ Å, $c = 18.365(3)$ Å, $\beta = 91.087(3)^\circ$, $V = 5067.5(15)$ Å³, $Z = 8$, $\text{fw} = 1008.06\text{ g mol}^{-1}$, $D = 2.643\text{ Mg m}^{-3}$, $T = 250\text{ K}$, $\mu = 17.45\text{ mm}^{-1}$, $\lambda(\text{Mo K}\alpha) = 0.71073$ Å, 9126 unique reflections, 449 parameters, $R[F^2 > 2\sigma(F^2)] = 0.0435$, $wR(F^2) = 0.1243$, $\text{GOF} = 1.009$. Crystal data for **2**: orthorhombic, $Iba2$, $a = 19.2519(17)$, $b = 8.7533(8)$ Å, $c = 11.9519(10)$ Å, $V = 2014.1(3)$ Å³, $Z = 4$, $\text{fw} = 951.95\text{ g mol}^{-1}$, $D = 3.139\text{ Mg m}^{-3}$, $T = 296\text{ K}$, $\mu = 21.944\text{ mm}^{-1}$, $\lambda(\text{Mo K}\alpha) = 0.71073$ Å, 3684 reflections, 1842 unique reflections, 82 parameters, $R[F^2 > 2\sigma(F^2)] = 0.0281$, $wR(F^2) = 0.0840$ (all data), $\text{GOF} = 1.086$.

(18) Lawton, S. J.; Rohrbaugh, W. J.; Kokotailo, G. T. *Inorg. Chem.* **1972**, *11*, 2227–2233.

(19) Naumann, D.; Tyrra, W.; Quadt, S.; Buslei, S.; Pantenburg, I.; Schafer, M. Z. *Anorg. Allg. Chem.* **2005**, *631*, 2733–2737.

(20) (a) Kudchadker, M. V.; Zingaro, R. A.; Irgolic, K. J. *Can. J. Chem.* **1968**, *46*, 1415–1424. (b) Liu, C. W.; Feng, C.-S.; Fu, R. -J.; Chang, H.-W.; Saillard, J.-Y.; Kahlal, S.; Wang, J.-C.; Chang, I.-J. *Inorg. Chem.* **2010**, *49*, 4934–4941.

(21) Moore, C. E. *Atomic Energy Levels*; National Bureau of Standards: Washington, DC, 1948; p 186.

(22) Krishnan, V.; Zingaro, R. A. *Inorg. Chem.* **1969**, *8*, 2337–2340.

is 0.17 μs , whereas the excited-state decay of compound **2** exhibited a biexponential process with lifetimes of 3.7 (50.8%) and 12.5 (49.2%) μs . The submicrosecond-to-microsecond lifetimes for both complexes suggest that the emissive states are triplet in nature. The excitation spectra for both complexes in the solid state at 77 K showed a broad band between 300 and 450 nm and a maximum at ~ 470 nm even though there is no absorption for both complexes in dilute solution extending over 370 nm.

Complex **1** shows a strong concentration-dependent emission in 2-MeTHF glass at 77 K. The clear vibrational structure of the emission spectrum with a maximum of 466 nm at 3.3×10^{-5} M became less resolved with the emission maximum red-shifted to 540 nm with a clear low-energy shoulder at 625 nm tailing to 700 nm at 3.3×10^{-3} M (Figure 2b). The excited-state decay monitored at 540 nm showed a biexponential process with lifetimes of 1.3 and 8.2 μs , whereas the decay monitored at 625 nm required an additional lifetime of 32.4 μs to fit the decay curve. Similar bathochromic shifts were also observed for excitation spectra (Figure S1 in the Supporting Information). The progressively bathochromic shift of emission and excitation spectra and the appearance of additional emission profiles upon increasing concentration are suggestive of closely lying emissive states of different origins. In addition, the excitation spectra of complex **1** (5.1×10^{-4} M) monitored at emission bands of 570 and 500 nm, respectively, show excitation bands at nearly the same positions but with different relative intensities (Figure S2 in the Supporting Information). This is in agreement with multiple emissive excited states under equilibrium. The high-energy emission profile observed at ca. 464 nm is tentatively assigned to a ligand-perturbed ^3MC transition, whereas the structureless low-energy emission profile observed at 540 nm is assigned to a $^3\text{LMCT}$ transition.²³ The aggregate structures may appear in high-concentration glass and in the solid state because of the strong aurophilic interaction, and the assignment of the low-energy emission profiles could also originate from the triplet ligand-to-metal–metal charge-transfer ($^3\text{LMMCT}$)²⁴ transitions with various degrees of gold(I)–gold(I) aurophilic interactions. Thus, the observed emission at different experimental conditions can be attributed to the different aggregate sizes with various degrees of aurophilically linked oligomers in frozen 2-MeTHF glass and in a solid at 77 K.

On the other hand, complex **2** displayed less concentration-dependent emission properties compared to complex **1** in 2-MeTHF glass at 77 K. The emission barely shifted from 620 nm at 2.0×10^{-5} M to 650 nm at 7.4×10^{-3} M (Figure S3 in the Supporting Information), which indicates notable molecular aggregates already existing at 77 K glass for complex **2**

even at concentration as low as 2.0×10^{-5} M. The excitation profiles also showed minor bathochromic shifts. The low-energy shift observed in the emission at 77 K for complex **2**, which has slightly shorter intra- and intermolecular Au \cdots Au distances, implies the influence of intra- and intermolecular Au–Au distances in the excited state. A similar emission energy shift was noticed for a gold(I) thiolate molecule, $[\text{AuS}_2\text{PPh}(\text{OC}_3\text{H}_9)]_2$, bearing shorter inter- and intramolecular Au–Au distances than those of analogous complexes $[\text{AuS}_2\text{PPh}(\text{OEt})]_2$ and $[\text{AuS}_2\text{PPh}(\text{OC}_3\text{H}_5)]_2$.^{3c} The arrangement of the digold entities is zigzag in complex **1**, with a Au–Au \cdots Au angle of 172.7° (av.), whereas the orientation of digold entities in complex **2** is linear, with a Au–Au \cdots Au angle of 180°. Thus, the less linear conformation in complex **1** diminishes the orbital overlap and results in a weaker aurophilic interaction in complex **1** than in complex **2**. The effect is to have complex **2** possess a higher degree of aggregation even at a low concentration and display less concentration-dependent emissive properties. Similar to the assignments for complex **1**, the orbital parentage of the emission from complex **2** is tentatively assigned to the $^3\text{LMCT}$ transition, with possible $^3\text{LMMCT}$ character at high concentration.

Complex **1** shows eminent solvent-dependent emission properties. For instance, the complex exhibits yellow luminescence with an emission maximum at 565 nm in THF, whereas the emission displays an orange color with a maximum at 595 nm in acetone. Interestingly, in dichloromethane glass, complex **1** ($\sim 10^{-2}$ M) shows vivid thermochromism with a color change from yellow (570 nm) to green (558 nm) upon an increase in the temperature from 77 to 177 K (Figure S4 in the Supporting Information). Similar thermochromism was observed in 2-MeTHF (Figure S5 in the Supporting Information). Although we could examine the luminescence of **2** in frozen CH_2Cl_2 (orange luminescence with $\lambda_{\text{em}}^{\text{max}}$ at 608 nm), its instability in other solvents such as acetone and THF and decomposition as the temperature is increased preclude further investigations.

In summary, the first structurally characterized dinuclear gold(I) compounds with each gold center linearly linked by two selenium atoms of the selenoorganophosphorus anion are reported. Besides, multiple emissions with orbital parentages of ^3MC , $^3\text{LMCT}$, and $^3\text{LMMCT}$ transitions derived from different aggregate sizes with various degrees of aurophilically linked oligomers in the solid state and frozen glass are revealed.

Acknowledgment. Financial support from the National Science Council of Taiwan (Grant NSC 97-2113-M-259-007) is gratefully acknowledged.

Supporting Information Available: X-ray crystallographic files in CIF format and synthesis and spectroscopic data (Table S1 and Figures S1–S5) for compounds **1** and **2**. This material is available free of charge via the Internet at <http://pubs.acs.org>.

(23) Crespo, O.; Gimeno, M. C.; Laguna, A.; Kulcsar, M.; Silvestru, C. *Inorg. Chem.* **2009**, *48*, 4134–4142.

(24) Yam, V. W. W.; Chan, C.-L.; Li, C.-K.; Wong, K. M.-C. *Coord. Chem. Rev.* **2001**, *216–217*, 173–194.